

*Real Time Simulation for Load Frequency
Control of Multisource Microgrid System
Using Grey Wolf Optimization Based
Modified Bias Coefficient Diagram Method
(GWO-MBCDM) Controller*

**Badal Kumar, Shuma Adhikari, Subir
Datta & Nidul Sinha**

**Journal of Electrical Engineering &
Technology**

ISSN 1975-0102

J. Electr. Eng. Technol.
DOI 10.1007/s42835-020-00596-2



Your article is protected by copyright and all rights are held exclusively by The Korean Institute of Electrical Engineers. This e-offprint is for personal use only and shall not be self-archived in electronic repositories. If you wish to self-archive your article, please use the accepted manuscript version for posting on your own website. You may further deposit the accepted manuscript version in any repository, provided it is only made publicly available 12 months after official publication or later and provided acknowledgement is given to the original source of publication and a link is inserted to the published article on Springer's website. The link must be accompanied by the following text: "The final publication is available at link.springer.com".



Real Time Simulation for Load Frequency Control of Multisource Microgrid System Using Grey Wolf Optimization Based Modified Bias Coefficient Diagram Method (GWO-MBCDM) Controller

Badal Kumar¹ · Shuma Adhikari¹ · Subir Datta² · Nidul Sinha³

Received: 26 February 2020 / Revised: 8 July 2020 / Accepted: 21 October 2020
© The Korean Institute of Electrical Engineers 2020

Abstract

This paper proposes a modified bias (MB) and coefficient diagram method (CDM) based PID controller as a first attempt in controlling frequency of a self-reliant microgrid (MG) system under extreme unfavourable scenarios. Recently developed meta-heuristic algorithm, Grey Wolf Optimizer (GWO), is used for optimizing the parameters of the proposed controller (GWO). Frequency deviation arises in the system due to active power mismatch between load power demand and actual power generation. In order to overcome this problem the CDM based gain values and frequency biased parameters of the MG system are used for determining the ranges of the control parameters for optimization with GWO which ensures that the search points generated by the search algorithm are stable ones. Simulation of the proposed GWO optimized MB-CDM controller-based MG system has been successfully implemented in real time simulation platform using digital simulator OPAL-RT. The performance of the system is obtained using proposed controller under different real-life scenarios and results are minutely analysed. The results are further compared with other relevant recent controllers including particle swarm optimization (PSO) MB-CDM controller to demonstrate that the proposed controller is superior to all other controllers. In addition, sensitivity analysis of the proposed controller for the MG system is studied under varying system parameters. The Simulink results illustrate that the proposed controller gives the best dynamic response amongst all other considered controllers in terms of peak transient deviation and settling time.

Keywords Self-reliant microgrid · Modern meta-heuristic algorithm · Modified bias and coefficient diagram method (MBCDM) controller

1 Introduction

In today's distribution system, the present passive distribution network can be converted into an active distribution network which usually operates in a grid connected mode by integrating the small-scale power generation. Nevertheless, these small-scale power systems must be disconnected from the main utility grid in the event of occurrence of a major fault in the main grid which may result in to cascade tripping and collapse of the grid. Hence, they can be operated as a separate system, called as isolated MG [1]. It is necessary to control the accuracy of the output of the micro-sources for balancing with the load demand of the MGs [2–4]. The DEG, AE, FC, BESS, FESS and gas turbine system etc. may be considered as governable sources in forming an MG system. If there is an active power difference between supply and load demand in any electrical system, that difference is become by the inertia of the system and thus the system

✉ Subir Datta
mzut168@mzu.edu.in

Badal Kumar
kumarbadal89@gmail.com

Shuma Adhikari
shumaadhikari@gmail.com

Nidul Sinha
nidul.sinha@gmail.com

¹ Department of Electrical Engineering, National Institute of Technology, Manipur, Imphal, India

² Department of Electrical Engineering, Mizoram University, Aizawl, Mizoram, India

³ Department of Electrical Engineering, National Institute of Technology, Silchar, India

frequency changes. In this scenario, the power output from the governable/controllable sources of the MG system must be regulated in such a way that it reduces the frequency deviations. This regulation is not linear due to generation rate constraint (GRC) and inherent time delay associated with the sources.

In [5], the power–frequency droop characteristics of MG system are introduced to regulate the frequency of the system and distribute the load among the MG sources. In [6] and [7], to improve the performance of frequency control and robustness in the existence of uncertainties, the robust H_∞ and μ synthesis PID parameters have been proposed for tuning the controller. In [8], the stability of the hybrid MG system, including MT (micro-turbine), FC and ES, were analyzed using fuzzy-based PI control strategy. In [8] and [9], meta-heuristic algorithms for optimization such as PSO based fuzzy logic and Kriging based global optimization with FO (fractional order) PID were implemented to regulate the deviation in frequency.

Traditional methods require a lot of trial and error efforts and this may result into sub-optimal solutions. Therefore, to achieve near global solution, an evolutionary algorithm is reported in [10] for finding fuzzy based controller gains. Several other optimization techniques: like Firefly Algorithm [11], Ant Colony optimization algorithm [12], Teaching Learning Based Optimization (TLBO) [13], Non-dominated sorting genetic algorithm-2 (NSGA-2) [14], Particle Swarm Optimization (PSO) [15], Differential Evolution (DE) [16] and [17], Hybrid Firefly Pattern Search (AHFPS) optimization technique [18], HBFOA–PSO algorithm [19], Gravitational Search Algorithm (GSA) [20], Selfish Herd Optimisation [21], Grasshopper Optimization Algorithm [22] and Multi-verse Optimizer (MVO) Algorithm [23] are effectively used to select the optimal parameters of the controller. Therefore, the suggestions of the use of modern techniques on the basis of meta-heuristic optimization algorithms are positively welcome to solve the real problems associated with MG system.

In [23], depicts introduction of MVO based fractional-order PID controller for regulating frequency of the micro-grid system. It is also observed that the proposed arrangement suffers from high peak deviation and setting time when subjected to extreme condition reason being that the controller was not validated under various real time scenarios. In [24], the modelling of MG and a PID controller based on LDR were presented to regulate its frequency. An open loop based Ziegler–Nichols technique (ZNT) was considered to determine the gain values of this controller. However, closed loop based ZNT cannot be applicable in time delay based first- or second-order systems. If closed loop based ZNT is chosen to control the frequency of the MG system then the tuning process will automatically be shifted to open loop based ZNT. Thus, it is observed that the scheme suffers from

high peak deviation under more stressed condition i.e. worst-case scenario. A modified bias based secondary controller was reported in [25] to achieve good dynamic frequency responses, but the cases of high stress conditions were not considered. In [26], another approach based on modified bias was proposed to design LDR, called MB-LDR, controller to get the optimal PID controller and bias parameters for regulating the frequency of the system under various operating scenarios with inclusion of worst scenario also. However, it also suffers from longer settling time, peak overshoot and a greater number of oscillations because LDR only considers open loop methods. Further, the stability of the open loop system is less than that of the closed loop system. Therefore, it is desirable to choose closed loop-based method like CDM technique for tuning of PID gain values [27, 28]. In order to obtain the desire responses of the system, CDM method can be used to determine the appropriate pole position of the closed loop transfer function [29]. It is an algebraic approach-based controller design method which includes simultaneous design of controller and attributes of polynomial. Thus, all the expressions are represented by polynomials of numerator and denominator, and this method yields the optimum results for cancellation of pole-zero [30]. This technique is also used in various applications of science and technology such as processes of bio-reactor [31], control of temperature [32], ball and beam systems [33], and process of heat exchanger [34] to improve the performance of closed loop systems. As far as the authors' knowledge, CDM based PID controller has not yet been used in multi-source MG system for regulation of frequency. In [35], the controller was designed with this method and also parameters are tuned to obtain the optimal values. But, CDM technique has certain limitations with respect to system parameters i.e. stability indices, settling time and stability limit index. However, the equivalent time constant ($\tau = t_s / (2.5 \sim 3)$), where t_s is the user specified settling time and the stability indices (γ_i) can be modified by the designer [36]. To get the appropriate value of stability index Routh-Hurwitz algorithm is applied on fourth and lower order generalized CDM equation. The stability index should also satisfy $\gamma_2 > \frac{1}{\gamma_1} + \frac{1}{\gamma_2}$ and $\gamma_1 \gamma_2 \geq 0$ conditions [37]. So, it requires tuning by the designer in various combinations for obtaining the optimal results, making it a time-consuming process. It is a time-consuming process to tune the number of variables using trial and error method and also it is not guaranteed that it will give universal global solution. However, meta-heuristic algorithms have proved to handle these types of optimization problems very efficiently. Further, the performance of meta-heuristic algorithms depends immensely on how fertile the regions they are made to search. In this sense here CDM based gain values become the guiding parameter for choosing the limits of the control variables for effective search.

In [38], a modern meta-heuristic method is proposed, called GWO, which is based on grey wolf's social cooperation and hunting activities to find and hunt a prey (solution) [39, 41]. As specific input parameters are not required for GWO implementation; GWO method becomes very popular as compare to other optimization algorithms. In GWO, three better categories of wolf have been assigned the same weight to estimate the next place of wolf in the procedure of iterations regardless of their capability.

The performance of the meta-heuristic algorithm depends hugely on how fertile the regions they are made to search within. Arbitrary choice of ranges for control variables will result into inefficient search and also there is possibility that there are a number of unstable (infeasible) search points. But, if CDM based gain values are considered for selection of appropriate ranges for the control variables for the meta-heuristic search algorithm which will ensure generation of stable (feasible) search points by the search algorithm and consequently result into better performance of the algorithm.

In this paper, a MBCDM based controller is proposed to control the frequency of a self-reliant MG system, as shown in Fig. 1, under different abnormal conditions and modern meta-heuristic technique, called GWO, is considered to determine the optimal gain values of the proposed controller. Moreover, OPAL RT-LAB (OP4510) is the digital simulator OPAL-RT that has also been used for validation of MG

system on real-time platform. The OPAL-RT lab based real time simulink procedures are explained in [40].

The key contributions of this work are as follows:

1. Design the proposed controller (i.e. MB-CDM Controller) and its gain and frequency bias parameters are optimized by GWO Algorithms.
2. Sensitivity analysis of the proposed controller with intelligently optimized gain and frequency regulation value to show the robustness of the controller to handle any type of uncertainty even worst/stressed case scenario.
3. The realistic performance of the proposed controller is validated on real time simulator platform OPAL RT-LAB (OP4510).

This paper has been organized as follows: the theoretical background of modelling of MG, deviation in power and frequency are provided in Sect. 2. Section 3 presents the modified bias (MB) based controller design. In Sect. 4 the design of CDM based controller gain is explained. Application of (MB-CDM) GWO based controller and its performance in MG is presented in Sect. 5. In Sect. 6, a comparative analysis of the controller parameter tuning based on traditional and evolutionary algorithms (GWO and PSO) is presented. Simulation results are presented in Sect. 7. Finally, the conclusions are drawn in Sect. 8.

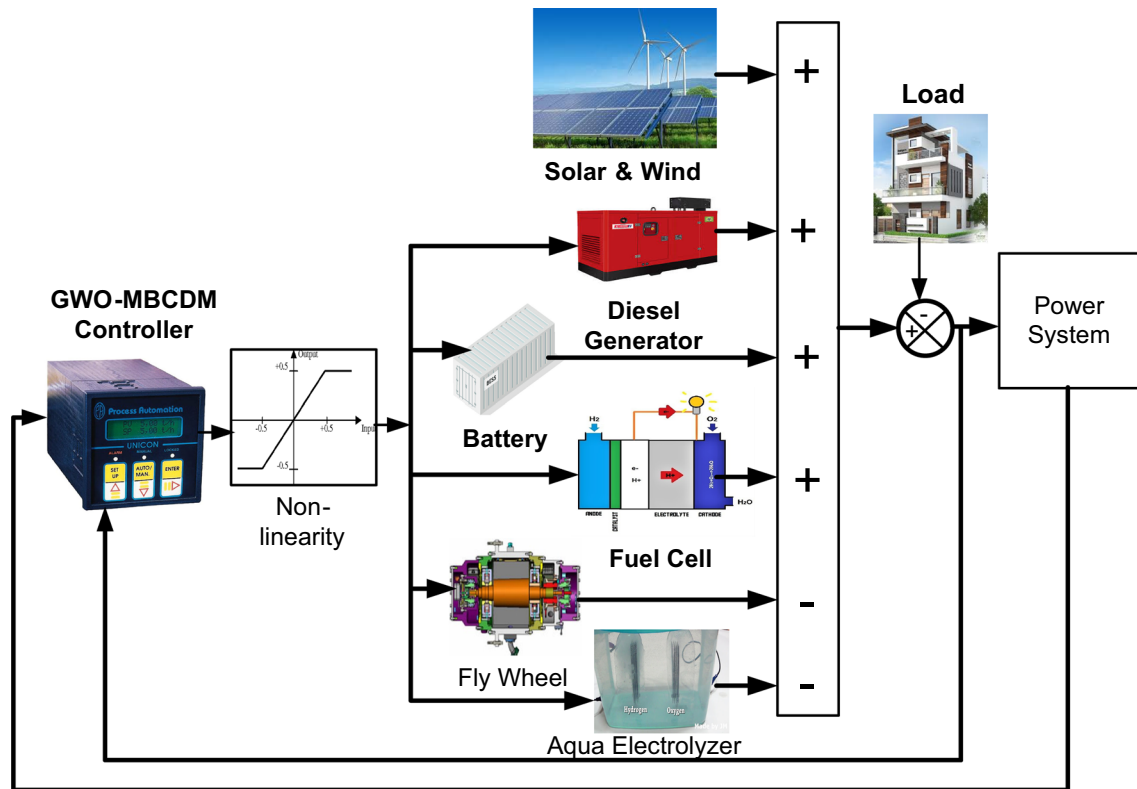


Fig. 1 Basic diagram of an islanded based MG system

2 Modelling of Proposed Hybrid System

Power generated from renewable energy resources (RERs) are usually fluctuating in nature. In order to store renewable power, the AEs and FC are incorporated in a MG. The hydrogen gas from AE can be accumulated in a hydrogen storage tank for use by the FC to produce electricity at any time and on demand. On the other hand, when the power generation from RES system becomes zero, the total energy has to be supplied by governable energy sources to fulfil the load demand. For adjusting their power during transient period, BESS and FESS can be considered for improving the attenuation of the frequency shift for each disturbance. Thus, assuming a 100% self-reliant islanded MG, the overall rating of the governable power supply is the same as the load rating. So, a MG system employed with ungovernable sources, loads (300 kW PV system, 400 kW WTG system, 700 kW load) and secondary governable sources (DEG, AE, FC, BESS and FESS and their ratings are 500 kW, 100 kW, 200 kW, 30 kWh and 30 kWh respectively) is considered in this paper and its block diagram is shown in Fig. 1.

2.1 Energies from Ungovernable Sources (Wind and Solar)

Typically, maximum power point tracking devices (MPPTs) are used for obtaining maximum energy from wind turbine conversion (WTC) and Solar photovoltaic (SPV) systems under varying wind velocity and solar radiation respectively. However, these units may not be adequate to control output power. Thus, in this paper, unmanageable sources (wind and sunlight) are treated as uncontrollable sources that are not involved in micro-grid frequency control. This paper uses a constant power strategy; details are reported in [24, 25]. Transfer functions of solar-PV and wind turbine system [7] are shown in Eq. (1) and (2) respectively.

$$G_{WT}(s) = \frac{1}{1 + sT_{WT}}, \quad (1)$$

$$G_{PV}(s) = \frac{1}{1 + sT_{PV}}, \quad (2)$$

where, T_{WT} and T_{PV} are the time constants of wind turbine and solar-PV units and their values are 1.5 s and 1.8 s respectively.

2.2 The Secondary Energy Sources (Governable Power Sources): Mathematical Analysis

In this section, governor and turbine transfer function of DEG, AE, FC, BESS and FESS obtained from [26] are shown below.

$$\left. \begin{aligned} G_{deg\ deg\ g}(s) &= \frac{1}{1 + sT_{deg\ deg\ g}}, G_{deg\ deg\ t}(s) = \frac{1}{1 + sT_{deg\ deg\ t}} \\ G_{ae}(s) &= \frac{1}{1 + sT_{ae}}, G_{fc}(s) = \frac{1}{1 + sT_{fc}} \\ G_{bess}(s) &= \frac{1}{1 + sT_{bess}}, G_{fess}(s) = \frac{1}{1 + sT_{fess}} \end{aligned} \right\} \quad (3)$$

where, $T_{deg\ deg\ g}$, $T_{deg\ deg\ t}$, T_{ae} , T_{fc} , T_{bess} and T_{fess} are time constants of governor and turbine of DEG, AE, FC, BESS, and FESS respectively. The system parameters are given in the Appendix.

2.3 Deviations in Power and Frequency

In an electrical system, which contains synchronous generators, if the quantity of load and generation power demand is not balanced, the system frequency will get disturbed [42, 43]. The power fluctuation is due to the difference between the amount of generation of power P_G and the amount of essential power demand P_L . From the synchronous machine's swing equation [38], the proposed mathematical model of the synchronous generator can be expressed as,

$$\Delta f = \frac{f_{sys}}{2Hs} [\Delta P_G - \Delta P_e], \quad (4)$$

here,

$$P_G = P_w + P_s + P_{deg} + P_{fc} - P_{ae} \pm P_{bess} \mp P_{fess} \quad (5)$$

where, P_w , P_s , P_{deg} , P_{ae} , P_{fc} , P_{bess} , and P_{fess} are wind power, solar energy, diesel power, aqua electrolyzer power, fuel cell power, battery power and flywheel power respectively.

In general, loads are mixed, such as frequency dependent and independent. The dynamic load characteristics of combined loads are approximated as follows.

$$\Delta P_e = \Delta P_L + D\Delta f. \quad (6)$$

Here, the first part of (6) does not depend on the frequency of the load, and the second part of (6) depends on the frequency of the load. Equation (7) can be derived using (4) and (6),

$$\Delta P_G - \Delta P_L = \left(\frac{2H}{f_{sys}} s + D \right) \Delta f. \quad (7)$$

Therefore, the mathematical expression of fluctuation in system frequency per unit deviation in power is shown as,

$$G_{sys}(s) = \frac{\Delta f}{\Delta P_G - \Delta P_L} = \frac{1}{D + (2H/f_{sys})s} = \frac{K_{hps}}{1 + sT_{hps}}, \quad (8)$$

here, K_{hps} (Gain of HPS) and T_{hps} (Time constant of HPS) are $1/D$ and $(2H/f_{sys} = M)$ respectively. D and M are damping and inertia constant of the power system. Here, it should be noted that (4) is only effective when MG has a synchronous machine.

3 Design of MB or Power-Frequency (p-f) Droop for MG System

In this sub-section, the key concepts of designing a P-f droop of a MG are considered. As the model and steps to design droop adopted in this section are the same as in [26], a brief explanation of this theme is provided to help the reader understand clearly. The P-f droop characteristics for different governable sources are related to each other as shown in (9).

$$R_{deg} : R_{fc} : R_{ae} : R_{bess} : R_{fess} = \frac{1}{P_{deg \text{ deg rated}}} : \frac{1}{P_{fcrated}} : \frac{1}{P_{aerated}} : \frac{1}{P_{bessrated}} : \frac{1}{P_{fessrated}}, \quad (9)$$

here, R_{dg} , R_{fc} , R_{ae} , R_{bess} and R_{fess} are the P-f droop coefficients; $P_{degrated}$, $P_{fcrated}$, $P_{aerated}$, $P_{bessrated}$ and $P_{fessrated}$ are the estimated power of DEG, FC, AE, BESS and FESS respectively. Because DEG has quadratic expressions, they can be unstable; the design procedure has been adopted taking this factor into consideration. A Signal flow graph (SFG) for closed loop of a DEG with an electrical system is shown in Fig. 2. The open loop transfer function of the DEG is given as,

$$G_{deg} = \frac{K_{hps}}{(1 + sT_{deg \tau})(1 + sT_{deg g})(1 + sT_{hps})}. \quad (10)$$

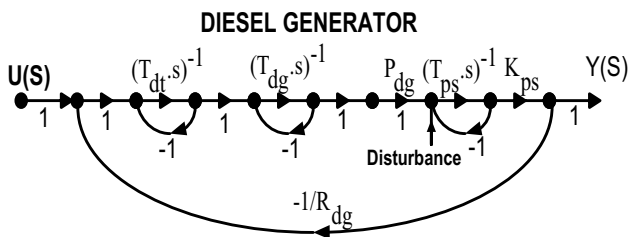


Fig. 2 SFG (signal flow graph) of the DEG

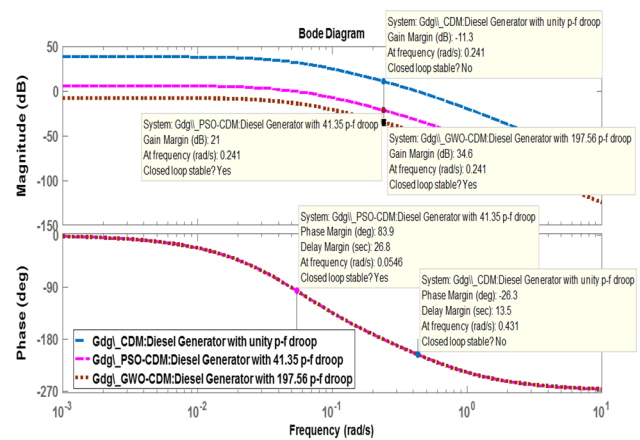


Fig. 3 Bode plot for DEG

Since Fig. 3 has a feedback path, characteristic equation of the closed loop system may be expressed by (11).

$$1 + G_{deg} \times \frac{1}{R_{deg}} = 1 + \frac{K_{hps}}{R_{deg}(1 + sT_{deg \tau})(1 + sT_{deg g})(1 + sT_{hps})}. \quad (11)$$

The bode plot of the DEG transfer function without p-f droop (G_{deg}) and with p-f droop ($G_{deg,dr} = G_{deg}/R_{deg}$) as shown in Eqns. (10) and (11) respectively are given in the Fig. 3. From Fig. 3, it can be concluded that a DEG with the characteristics of "unity" droop makes electrical system unstable by displaying negative phase margin and gain margins [40]. However, with 41.35 and 197.56 Hz/pu p-f droop the system is stable. It can be guaranteed from the positive margins. Now, the p-f droop of AE (100 kW), FC (200 kW), BESS (30 KWh) and the FESS (30 KWh) can be drawn using Eq. (9). In our case, these values are 0.012, 377.34, 0.0011 and 0.0004 respectively. In the Bode diagram is shown in Fig. 3, positive phase margin and gain margin indicate that all secondary systems are stable. It gives the value of droop co-efficient.

4 Design of CDM Based Controller Parameters of a MG System

In this work, we will consider only the third-order model of a diesel engine generator and the second order model of the remaining secondary controllable power sources at this stage.

Figure 4 shows a CDM control based single-input single-output (SISO) linear time-invariant system. In Fig. 4, presented below "r", "u", "d" and "y" are treated as reference signal, controller signal, disturbance signal and the output

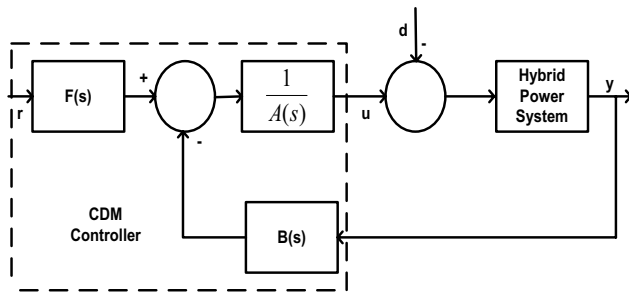


Fig. 4 Standard block diagram of CDM control System

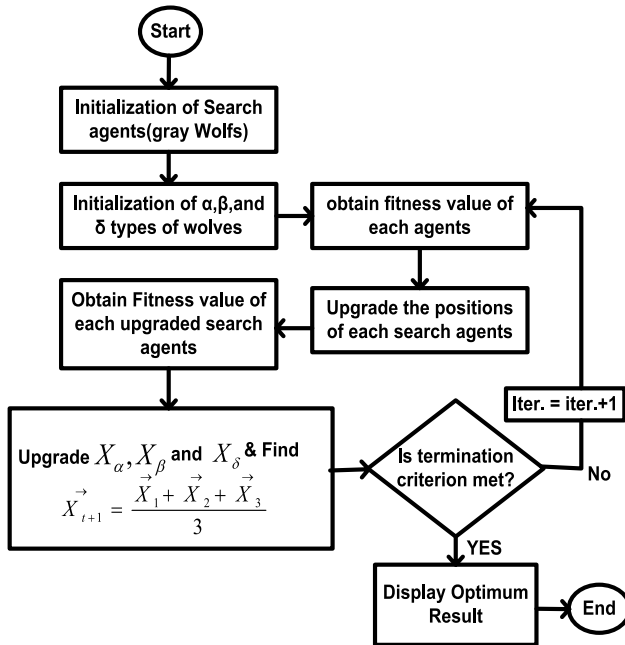


Fig. 5 GWO algorithm flowchart

of the control system respectively. Next, when evaluating the performance of the entire design, restore the resonant mode. Design procedure for PID controller with CDM is verified through MATLAB. Therefore, in our design we first use the following simplified model of the MG plant. Plant transfer function is,

$$G_p(s) = \frac{D}{As^3 + Bs^2 + Cs + 1}. \quad (12)$$

And PID Transfer Function is,

$$G_c(s) = K_p + \frac{K_I}{s} + K_D s. \quad (13)$$

Now Close Loop Transfer Function is,

$$G_{cl}(s) = 1 + G_p(s) \times G_c(s) = 0. \quad (14)$$

As a simplification, the characteristic equation of the closed-loop transfer function is,

$$P_{cl}(s) = As^4 + Bs^3 + (C + DK_D)s^2 + (1 + DK_P)s + DK_I. \quad (15)$$

In the CDM method, substitute the stability index $\gamma_1, \gamma_2, \gamma_3$ and the equivalent time constant τ . Therefore, the $P(s)$ can be expressed as,

$$P(s) = a_4 s^4 + a_3 s^3 + a_2 s^2 + a_1 s + a_0 \quad (16)$$

$$\text{where, } a_i = \frac{a_0 \tau^i}{(\gamma_{i-1} \gamma_{i-2}^2, \dots, \gamma_2^{i-2}, \gamma_1^{i-1})}.$$

Equalizing $P(s)$ as above with $P_{cl}(s)$ of the plant in (15), the parameters of PID controller are received for all the secondary sources.

5 Application of GWO for the Optimization of Parameters of MB-CDM Based Controller of MG System

If the controller is used on electrical power system, it should be optimal for all criteria, including system robustness, dynamics, and so on. Thus, the controller performance is checked using various objective functions.

From an optimization point of view, the objective function helps to generate a dynamic response with minimal overshoot and settling time. With this in mind, the ISE criterion is used in this work as an objective function for the evaluation of dynamic responses based on minimal settling time and minimal overshoot.

Table 1 PID controller gains tuned with MB-LDR Method [27]

Components of MG	MB K_f	LDR K_p	LDR K_i	LDR K_d
DEG	20.4918	0.1025	0.0073	0.3013
AE	0.002	1.498	4.5399	0.1044
FC	40.9836	0.1858	0.0464	0.156
BESS	0.001	3.38	0.1251	0.098
FESS	0.001	3.38	0.1251	0.098

Table 2 PID controller gains tuned with MB-CDM1 method (for standard values of gamma i.e. $\gamma_1 = 2.5, \gamma_2 = 2, \gamma_3 = 2$)

Components of MG	MB K_f	CDM K_p	CDM K_i	CDM K_d
DEG	20.4918	0.215	0.01384	1.02517
AE	0.002	1.2401	1.9813	0.1141
FC	40.9836	0.08187	0.0091	0.1395
BESS	0.001	0.017637	7.7614	0.1131
FESS	0.001	0.017637	7.7614	0.1131

Table 3 PID controller gains tuned with MB-CDM2 method (for chosen values of gamma i.e. $\gamma_1 = 2.75$, $\gamma_2 = 2.25$, $\gamma_3 = 1.5$)

Components of MG	MB K_f	CDM K_p	CDM K_i	CDM K_d
DEG	20.4918	0.346	0.0235	1.51
AE	0.002	1.69	2.70	0.1892
FC	40.9836	0.1158	0.0123	0.2317
BESS	0.001	3.3498	10.56	0.1878
FESS	0.001	3.3498	10.56	0.1878

Table 4 PID Controller (MB-CDM) Gains Tuned with PSO Algorithm

Components of MG	MB-PSO K_f	CDM-PSO K_p	CDM-PSO K_i	CDM-PSO K_d
DEG	113.65	1.9899	0.0989	2.2713
AE	0.0257	0.1001	2.5684	0.0108
FC	3.9786	0.8332	0.0901	1.5
BESS	0.0171	0.1033	2.4603	1.1998
FESS	0.0194	0.1243	77.6321	1.1680

$$ISE = \int_0^T |\Delta f \times \Delta f|^2 dt, \quad (17)$$

here, Δf is a deviation of MG frequency; T is the simulation time.

At this section, the GWO algorithm has been employed for solving the problem associated with the system of MG. The algorithmic stages of the implemented technique are listed below.

Stage 1: According to the input parameters (such as the search agents, size of population, control variables etc.) of the GWO algorithm and the structure of the controller, the search space limits (both lower and upper limits), the number of elitism parameters and the total number of generations are initialized.

Stage 2: In the initial procedure, search agents or grey wolves (i.e. controller parameters like (K_p , K_i , K_d and regulation parameter K_f are arbitrarily produced between the upper and lower limits from the space of search).

Stage 3: Estimate the fitness and identify α , β , and δ wolves in the search space based on fitness.

Stage 4: Upgrade the positions of the GW variables (α , β , δ) by using the pseudo code is as given below;

```

For i=1: searchagent_no
    if fitness < alpha
        alpha ← upgrade    fitness
    finish
    if fitness > alpha && fitness < beta
        alpha ← upgrade    fitness
    finish
    if fitness > alpha && fitness > beta && fitness < delta
        alpha ← upgrade    fitness
    finish
finish
    
```

Stage 5: Define two random numbers r_1 , r_2 between $[0, 1]$ and \vec{a} linearly from 2 to 0.

Stage 6: Upgrade the location of search agents that contain Omega. And finally, change the control variables (K_p ; K_i ; K_d and K_f) for each search agent.

Stage 7: Check to see if the search agent has exceeded the search space, and non-feasible solutions can be replaced with an arbitrarily produced possible solution set.

Stage 8: Arrange the position of the search agents found in step 6 from the best value to the worst value and utilize it for the next generation.

Stage 9: Go back to step 4 and continue the process until the final criteria are met.

A regular flow chart of the GWO technique is depicted in Fig. 5 and for more detailed description of the GWO technique the reader may refer to [38].

Table 5 PID controller (MB-CDM) gains tuned with GWO algorithm

Components of MG	MB-GWO K_f	CDM-GWO (K_p)	CDM-GWO (K_i)	CDM-GWO (K_d)
DEG	489.43	14.0503	0.0714	9.7289
AE	0.0055	0.1010	18.90	0.0212
FC	76.362	0.8712	0.0213	0.0103
BESS	0.0008	0.008989	0.10205	0.4171
FESS	0.0047	0.01025	593.0858	0.6009

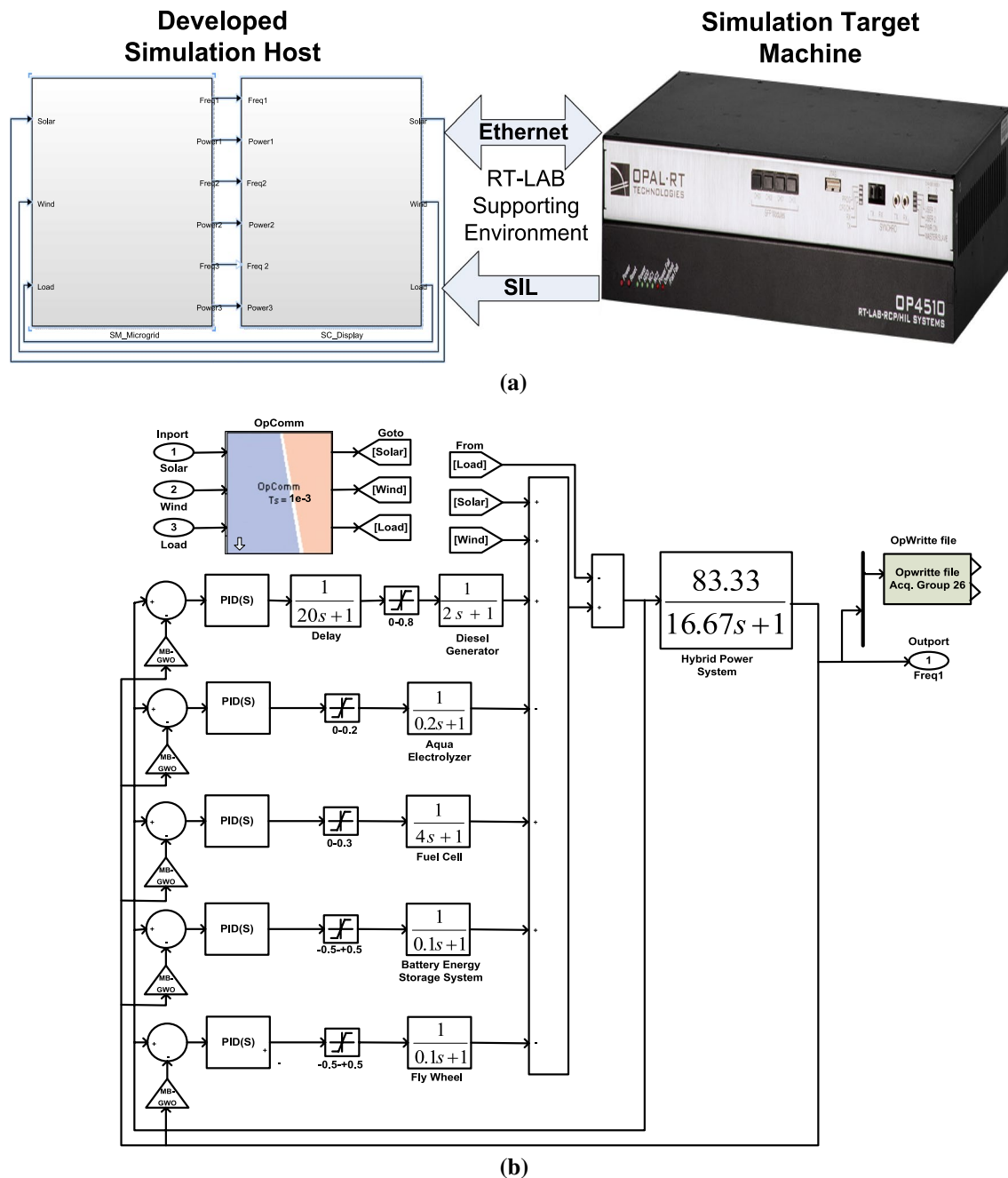


Fig. 6 a Structural diagram of RT-Lab system and b Simulink block diagram of the MG system in Opal-RT platform

6 A Comparative Analysis of Tuning of Controller Parameters

The main purpose of the controller is to reduce the deviation of frequency by controlling the power output of the secondary power supply and to generate an appropriate control signal for improving the system performance.

In the existence of many secondary energy sources, there is a possibility of undesirable interaction between those

regulators leading to the disturbance in frequency of MG. So far, there is not a single definition for application of optimal tuning methods to all loops. As a result, individual PID controller must properly be tuned to avoid adverse interactions [25]. The values of all the parameters (K_p , K_i , K_d and frequency bias- K_f) of MB-LDR Method are taken from [26, 40]. In CDM, the controller gain values K_p , K_i and K_d were obtained from coefficient diagram method [27] and change in the parameter of frequency regulation from Bode plot

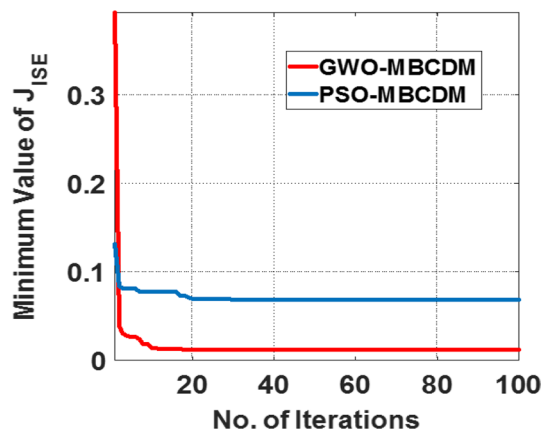
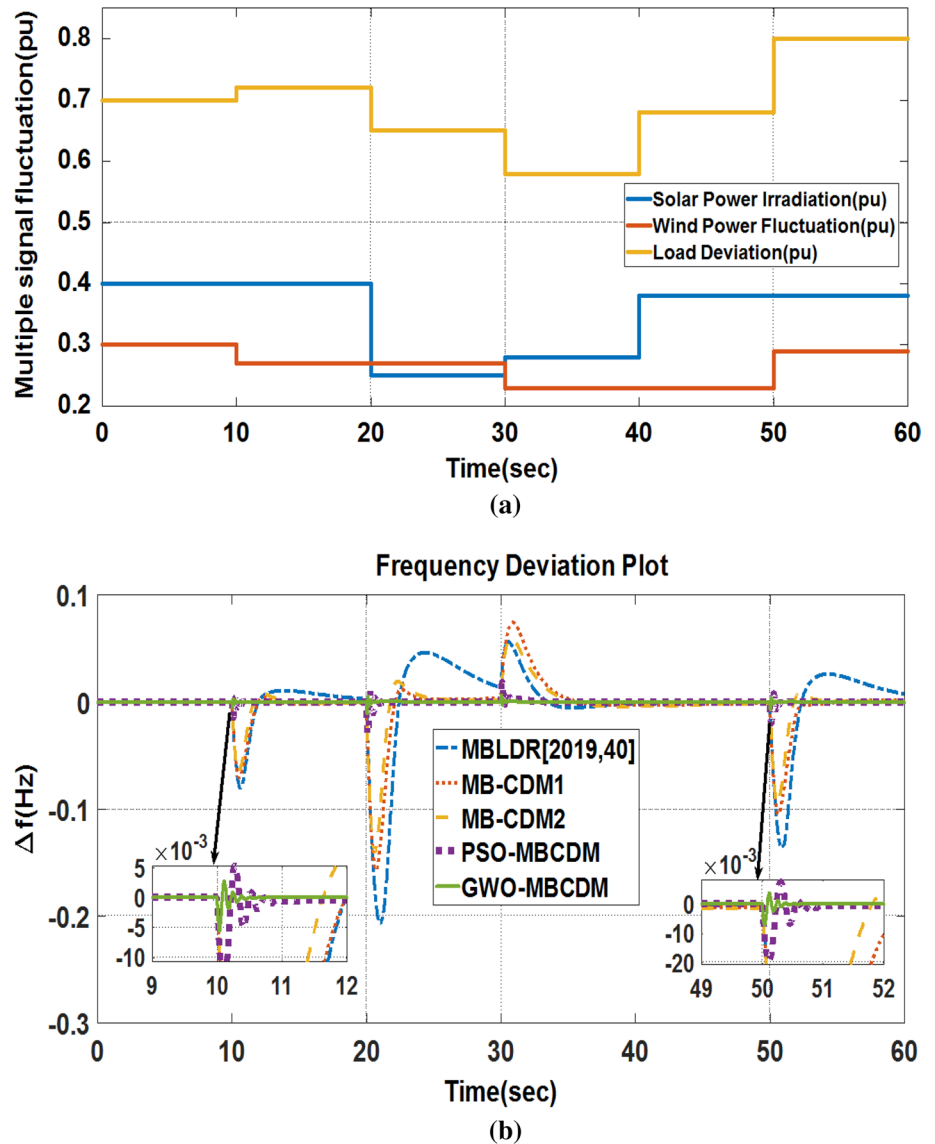


Fig. 7 Convergence characteristics of the **a** GWO-MBCDM and **b** PSO-MBCDM algorithms

Fig. 8 Results for Scenario-1, **a** power variations in multiple sources and load and **b** frequency responses in MG



stability criterion [26]. In this paper, all the optimal parameters of the proposed controller are computed using PSO and GWO for comparison.

The frequency regulation parameter and the PID controller gain values are computed by using MB-LDR, MB-CDM1, MB-CDM2, PSO-MBCDM and GWO-MBCDM methods are given in Tables 1, 2, 3, 4 and 5 respectively.

Simulation results of the system (Fig. 6) are obtained using the different set of gain values of PID controller as given in Table 1, 2, 3, 4 and 5 and their responses are compared. The convergence characteristics of GWO-MBCDM and PSO-MBCDM has depicted in the Fig. 7.

Table 6 Range of settling time and peak deviation of the MG's frequency under all the test scenarios

Cases	Controller	Settling time (s)	Peak deviation range	Remarks
Scenario-1	MBLDR	12–15	−0.22 to 0.055	From Fig. 7b
	MB-CDM1	8–9	−0.16 to 0.06	Good response
	MB-CDM2	5–8	−0.14 to 0.057	Better than MB-CDM1
	PSO-MBCDM	2–3	−0.03 to 0.018	Better response
	GWO-MBCDM	0.5–1	−0.011 to 0.006	Best response
Scenario-2	MB-LDR	55	−5.2 to 3.2	From Fig. 8b
	MB-CDM1	40	−4.6 to 1.9	Good response
	MB-CDM2	39	−4.4 to 1.7	Better than MB-CDM1
	PSO-MBCDM	5	−0.51 to 0.45	Better response
	GWO-MBCDM	3	−0.47 to 0.45	Best response
Scenario-3	MB-LDR	13–17	−0.51 to 0.12	From Fig. 9b
	MB-CDM1	8–15	−0.35 to 0.11	Good response
	MB-CDM2	5–14	−0.31 to 0.085	Better than MB-CDM1
	PSO-MBCDM	2–4	−0.07 to 0.03	Better response
	GWO-MBCDM	1–2	−0.026 to 0.014	Best response
Scenario-4	MB-LDR	60–65	−0.04 to 0.022	From Fig. 10b
	MB-CDM1	55–65	−0.035 to 0.035	Good response
	MB-CDM2	50–65	−0.031 to 0.029	Better than MB-CDM1
	PSO-MBCDM	25–30	−0.007 to 0.0065	Better response
	GWO-MBCDM	2–10	−0.0029 to 0.0025	Best response

7 Experiments and Analysis of Results

Figure 6 is modelled in the MATLAB/SIMULINK (R2018b) environment and also implemented in OPAL-RT environment for real-time simulation [41]. The MG system is run for 60 s to study the performance of the MG system and for analyzing the results in details by subjecting the system to power variation both at load and source ends. In the beginning, it is considered that the MG system has WTG, solar PV and load.

Wind and solar systems supply constant powers of 0.3 pu and 0.4 pu respectively and load demand is considered as 0.7 pu before the occurrence of any type of disturbances. The simulation of the study model is performed on Intel, core i-7 C.P.U with 3.4 GHz and 8 GB RAM computer. In this paper, 30 population size and 50 numbers of iterations are considered for the GWO method. The optimization algorithm runs 10 times independently and the best optimum results are used as PID controller parameters. Results, obtained using GWO based MB-CDM controller are compared with that of obtained with PSO based MB-CDM, MB-CDM1, MB-CDM2 and MB-LDR controllers and it is found that the proposed controller gives the best responses amongst all the four controllers.

7.1 Performance of the System for Different Scenarios

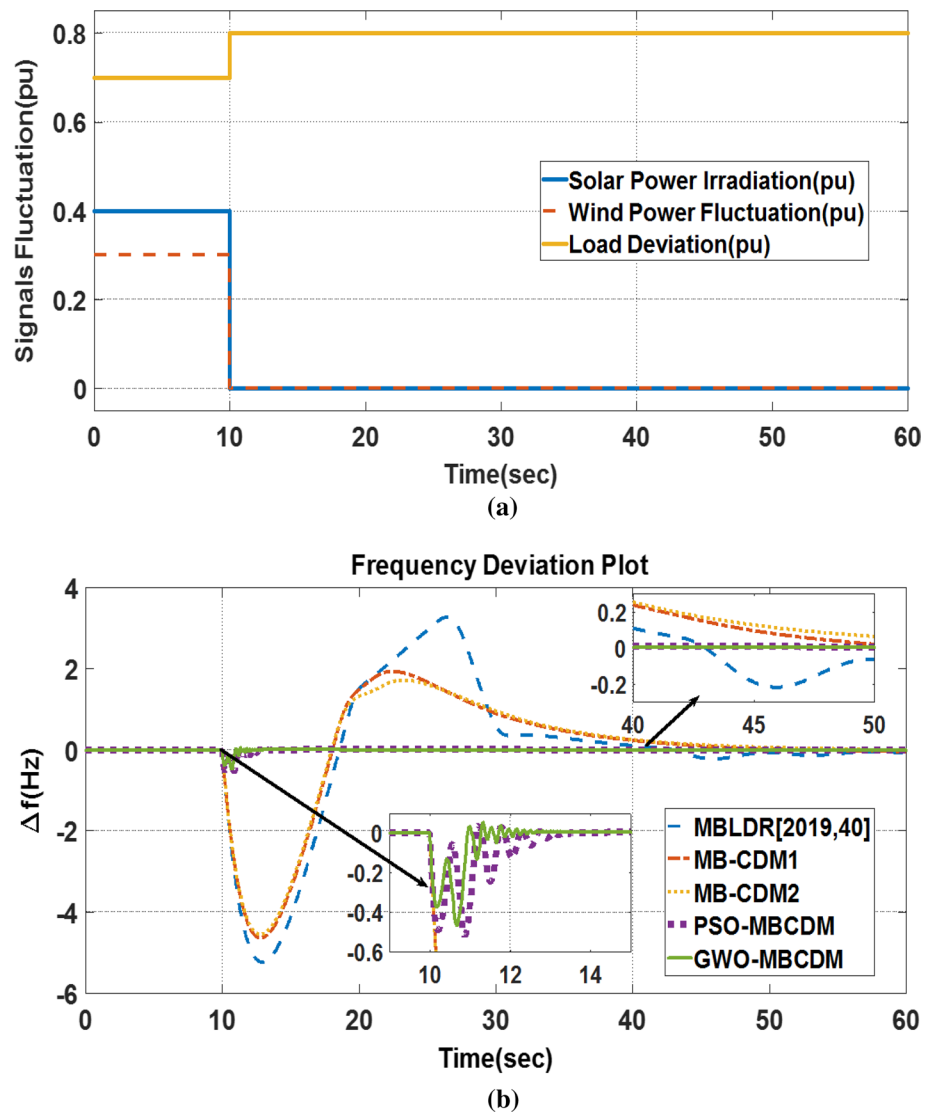
Four scenarios are considered, in this paper to study the effectiveness of the proposed GWO-MBCDM controller during penetration of renewable generations in a microgrid system, as shown in Fig. 6.

7.1.1 Scenario-1: Practical Condition (Simultaneous Fluctuations in Solar Power, Wind Power and Load)

In this scenario the proposed controller based MG system is subjected to a combination of solar power, wind power and load disturbances simultaneously as shown in Fig. 8a. The load frequency responses of the MG under this practical condition are depicted in Fig. 8b.

From Fig. 8b, it is noticed that the settling time of the responses using MB-LDR, MB-CDM1, MB-CDM2, PSO-MBCDM and GWO-MBCDM controllers are 12–15 s, 8–9 s, 5–8 s, 2–3 s and 0.5–1 s respectively and also the range of Peak deviations using these controllers are (−0.22 to 0.055), (−0.16 to 0.06), (−0.14 to 0.057), (−0.03 to 0.018) and (−0.011 to 0.006) respectively and the details are mentioned in Table 6.

Fig. 9 Results for Scenario-2, **a** power variations in sources and load and **b** frequency responses in MG



Therefore, it can be observed from the simulation results as shown in Fig. 8b that the dynamic responses achieved with the proposed GWO-MBCDM controller are better than that of other controllers in terms of peak transient deviation and settling time followed by the PSO-MBCDM controller. All the dynamic responses of the system obtained using any MB-CDM controller are better than that of MB-LDR controller.

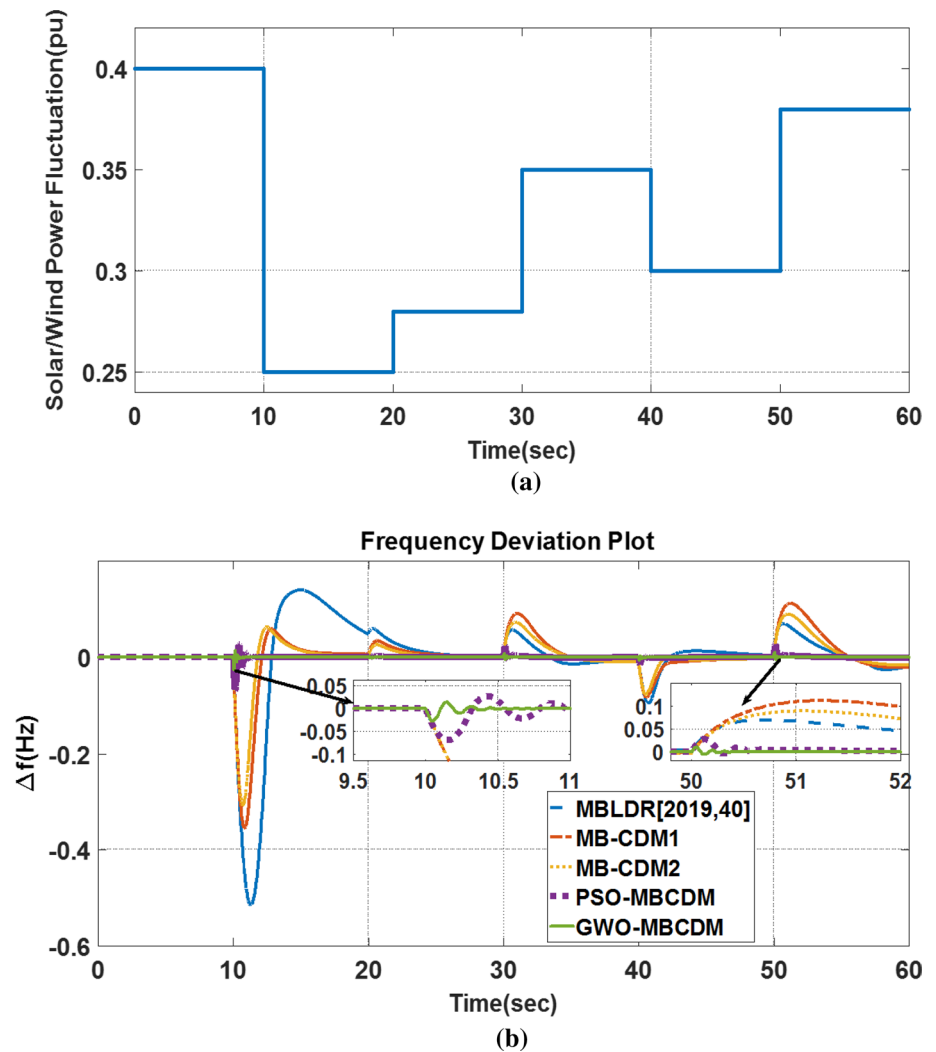
7.1.2 Scenario-2: Worst Case Scenario (Simultaneous Fluctuation in Solar Power, Wind Power and Load)

In this case, power from wind and solar are changed from 0.3 pu and 0.4 pu to 0 pu at 10 s to create worst condition, and

also the load power demand is increased to 0.8 pu from 0.7 pu at 10 s as illustrated in Fig. 9a. Due to the sudden change in the load and generation, the MG (especially secondary source) experiences a large deviation in frequency as shown in Fig. 9b. So, to minimize the frequency deviation and its oscillations, the output power of the MG is regulated by the optimized controllers.

Frequency responses of the MG system under this scenario which are obtained by using MB-LDR, MB-CDM1, MB-CDM2, PSO-MBCDM and the proposed GWO-MBCDM controllers is shown in Fig. 9b. The settling time and peak deviation of the frequency of the MG obtained using these controllers are given in Table 6. It can be

Fig. 10 Results for Scenario-3, **a** variations in solar/wind power and **b** frequency responses in MG



observed from Fig. 9b and Table 6 that the proposed controller, based on GWO based MB-CDM, provides the best dynamic behaviour amongst all the controllers considered in terms of peak deviations and settling time followed by PSO-MBCDM controller. All the MB-CDM controllers give better response than MB-LDR controller.

7.1.3 Scenario-3: Fluctuations in Solar Power ($\Delta P_{\text{solar/Wind}}$)

In this scenario, the value of irradiation of the sun is gradually changed, as shown in Fig. 10a, at time 10 s, 20 s, 30 s, 40 s and 50 s. The frequency responses of the controllers in the system under variation of solar irradiation are obtained and shown in Fig. 10b and in Table 6.

The simulation result (Fig. 10b) shows that the dynamic performance of the proposed GWO-MBCDM controller provides the best amongst all the controllers followed by PSO-MBCDM in terms of peak transient deviation and

settling time and the details are mentioned in Table 6. It can be observed that all the MBCDM controllers are better than the MB-LDR controller.

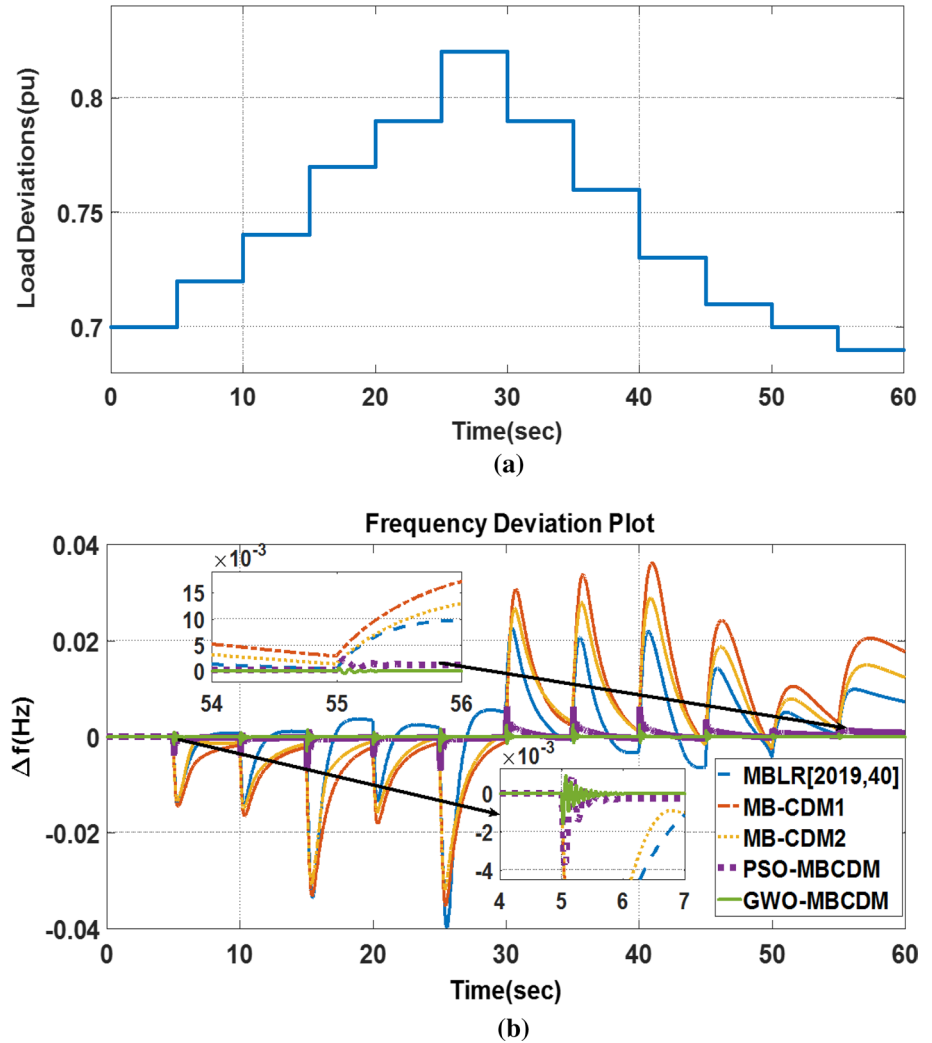
7.1.4 Scenario-4: Load Fluctuations (ΔP_{Load})

In this section, the load of the MG system is varied in step pattern, from time 5 to 55 s, as shown in Fig. 11a. The frequency responses of the MG system under the variation of step pattern-based load is obtained using MB-LDR, MB-CDM1, MB-CDM2, PSO-MBCDM and proposed GWO-MBCDM based controllers are as shown in Fig. 11b.

The values of settling time and peak deviation of the frequency of the MG under this scenario are also presented in Table 6.

From the simulation results as shown in Fig. 11b it can be noticed that the frequency responses of the study system obtained using the proposed GWO-MBCDM is the best

Fig. 11 Results for Scenario-4, **a** power variations in load and **b** frequency responses in MG



amongst all the considered controllers in terms of settling time and peak transient deviations followed by the PSO-MBCDM controller.

In all the four test scenarios, the performance of the system using GWO based MB-CDM based proposed controller is the best amongst all the considered controllers in terms of peak transient deviation, settling time and number of oscillations. The PSO-MBCDM controller is better from the rest. All the MB-CDM controllers give better performance than MB-LDR controller. Further, the performance of the proposed controller optimized in scenario 1 when subjected to wide variation in load as well as in generation (solar and wind) demonstrate its high robustness as compared to other controllers.

7.2 Sensitivity Analysis

To examine the robustness of the designed proposed controller sensitivity analysis is carried out by dynamic analysis of the proposed system with the proposed controller optimized under normal conditions while varying the system parameters and system operating conditions. The system parameters like D , T_{deg} , T_{degr} , etc. are changed within the range of $\pm 50\%$ in steps of 25% and the performance of the proposed controller is analyzed for the worst case scenario. Analyzing the controller performance under worst case helps us in estimating its robustness under other healthier conditions. Table 7 depicts the fitness value (ISE), the maximum deviation of frequency and power and it can be noticed that the variations are within

Table 7 Sensitivity analysis of the micro-grid system with (MB-CDM) GWO

Parameter	% of Change	ISE Value	Maximum Deviation	
			Δf	ΔP
Nominal	0	0.011663	0.0335	0.3954
D	+50	0.011594	0.04787	0.41619
	+25	0.011745	0.0475	0.4175
	-25	0.01254	0.04588	0.40883
	-50	0.0073787	0.03726	0.4035
M	+50	0.0052757	0.032567	0.41885
	+25	0.007556	0.038037	0.41822
	-25	0.02172	0.06775	0.414998
	-50	0.04569	0.09345	0.41492
K	+50	0.0026257	0.0198	0.40948
	+25	0.0046308	0.01355	0.4034
	-25	0.05378	0.04427	0.38565
	-50	13.3697	0.1621	0.313505
T_{deg}	+50	0.018871	0.056	0.43672
	+25	0.014936	0.0491	0.41315
	-25	0.0092801	0.07894	0.44323
	-50	0.0070586	0.01022	0.37982
T_{degt}	+50	0.012139	0.05	0.41669
	+25	0.011694	0.04815	0.41653
	-25	0.011735	0.05027	0.420005
	-50	0.01164	0.049765	0.41885
T_{fc}	+50	0.013247	0.04988	0.40865
	+25	0.0122	0.04977	0.41496
	-25	0.011308	0.04617	0.41447
	-50	0.016156	0.05257	0.41796
T_{ae}	+50	0.011703	0.04904	0.417092
	+25	0.011738	0.04964	0.417498
	-25	0.011657	0.04751	0.41768
	-50	0.011666	0.04662	0.41853
T_{bess}	+50	0.010783	0.02292	0.3666
	+25	0.010675	0.034638	0.39924
	-25	0.028232	0.050042	0.44775
	-50	0.028162	0.034403	0.5257
T_{fess}	+50	0.022123	0.05465	0.4329
	+25	0.016636	0.052655	0.413125
	-25	0.0073787	0.03587	0.39503
	-50	0.0037458	0.01572	0.35624

acceptable limit and frequency deviation of all tests are under 0.2 Hz. From the observations, it can be deduced that the proposed GWO optimized MB-CDM based PID controller is sufficiently robust and is capable of controlling frequency

even in worst situations whilst the system experiences wide variations in load as well as in solar and wind power connected to the MG.

Further, the deviation in frequency and power are given in Table 7 when the system is subjected to change in its parameters within the range of $\pm 50\%$. Figure 12a and b show the frequency responses of the MG system due to the variation of damping co-efficient (D) and fuel cell time constant (T_{fc}) respectively under worst case situation. It can be observed from Fig. 12a, b and Table 7 that the maximum deviation of frequency is lower than 0.2 Hz indicating that the proposed controller with optimal parameters obtained in normal operating conditions gives considerably satisfactory results for LFC of MG system.

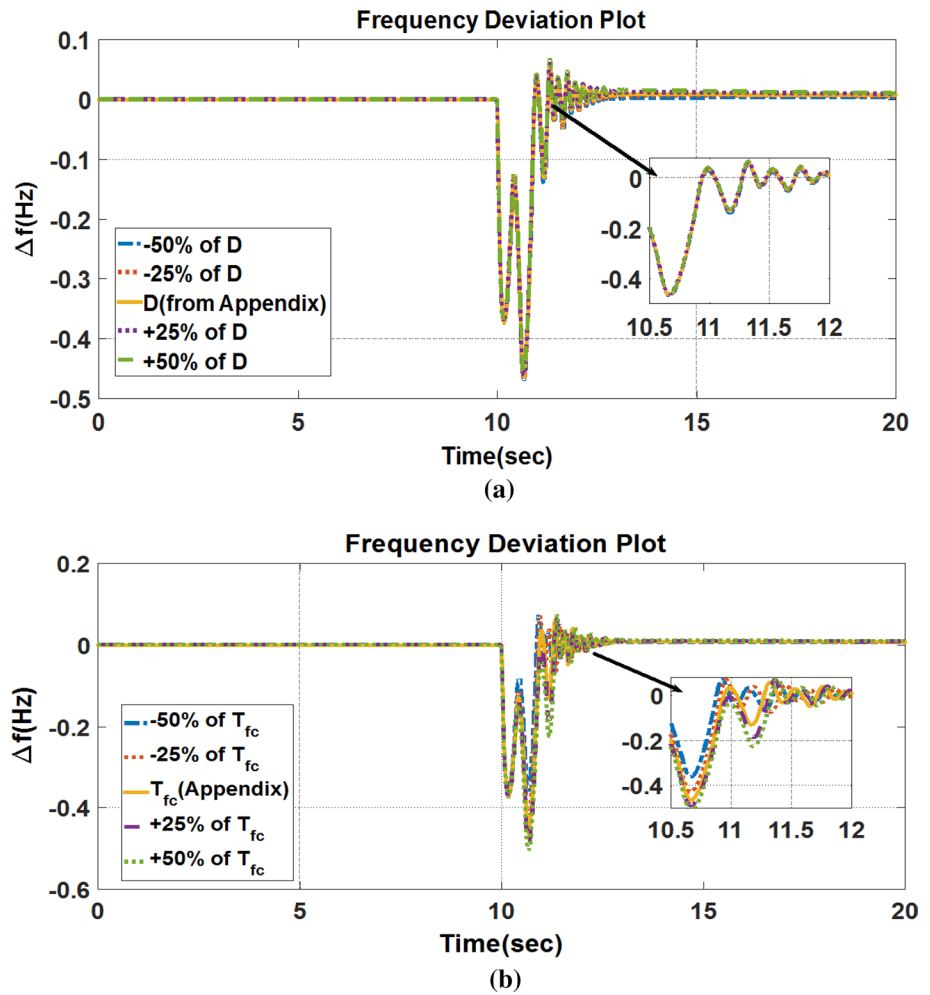
8 Conclusion

The load frequency control of MG integrated with renewable energy sources is studied. A modified bias (MB) and coefficient diagram method (CDM) based PID controller is proposed for the first time for regulating the frequency of a self-reliant microgrid (MG) system. A recent meta-heuristic algorithm GWO is also considered to compute the optimal parameters of the proposed controller to get improved responses of the MG system. In addition, the GWO based MB-CDM controller is also implemented in OPAL-RT digital simulator based real-time simulation environment to validate the realistic performance of the MG system under different scenarios including the worst case.

The real-time experimental results obtained using GWO based MB-CDM controller are compared with those obtained using other controllers like PSO based MB-CDM, MB-CDM, and MB-LDR controllers. It is observed, from responses of the system, that the GWO based MB-CDM controller gives the best results particularly in terms of peak transient deviation, settling time, and number of oscillations and the stability of MG thus proving that the proposed controller yields the best dynamic performance.

Furthermore, the sensitivity analysis is also carried out with the variation of system parameters to study the robustness of the proposed controller optimized at normal conditions. Results show that the proposed controller produces satisfactory results even with variation of different system parameters demonstrating the proposed controller optimized at normal conditions is robust enough and need not be re-tuned with the variation of system conditions.

Fig. 12 Sensitivity analysis of the proposed GWO-MBCDM controller for worst case under the **a** variation of D and **b** variation of T_{fc}



Acknowledgements We take this opportunity to offer our wholehearted gratitude to TEQIP-III project for making available OPAL-RT Loop Simulator at NIT Manipur which assisted us to validate all responses of the proposed controller based MG system in real time environment.

Appendix

Nominal parameters of the MG:

$f_{sys} = 50$ Hz, $P_{base} = 1$ MVA, $D = 0.012$ MW/Hz, $M = 0.2$ s, $T_{degg} = 2$ s, $T_{degt} = 20$ s, $T_{fc} = 4$ s, $T_{ae} = 0.2$ s, $T_{bess} = 0.1$ s, $T_{fess} = 0.1$ s, $K_{degg} = K_{degt} = K_{ae} = K_{bess} = K_{fess} = 1$, $T_{WT} = 1.5$ s, $T_{PV} = 1.8$ s, $K_{WT} = K_{PV} = 1$.

References

- Hassan B (2009) Robust power system frequency control, 2nd edn. Springer, Berlin
- Shankar R, Chatterjee K, Chatterjee TK (2015) Coordination of economic load dispatch and load frequency control for interconnected power system. J Inst Eng India Ser B 96(1):47–54
- Gemine Q, Ernst D, Cornelusse B (2017) Active network management for electrical distribution systems: problem formulation, benchmark, and approximate solution. Optim Eng 18(3):587–629
- Balaguer IJ, Lei Q, Yang S, Supatti U, Peng FZ (2011) Control for grid-connected and intentional islanding operations of distributed power generation. IEEE Trans Ind Electron 58(1):147–157
- Majumder R, Chaudhuri B, Ghosh A, Majumder R, Ledwich G, Zare F (2010) Improvement of stability and load sharing in an autonomous microgrid using supplementary droop control loop. IEEE Trans Power System 25(2):796–808
- Al-Muhanna A, Al-Nujaimi A, Al-Baiyat S (2017) Robust H_∞ and μ -Synthesis frequency control for two-bus islanded microgrid. Saudi Arabia Smart Grid SASG, Jeddah, pp 1–9
- Bevrani H, Feizi MR, Ataee S (2016) Robust frequency control in an islanded microgrid: H_∞ and μ -synthesis approaches. IEEE Trans Smart Grid 7(2):706–717
- Shokoohi S, Golshannavaz S, Khezri R, Bevrani H (2018) Intelligent secondary control in smart microgrids: an on-line approach for islanded operations. Optim Eng 19(4):917–936

9. Pan I, Das S (2015) Kriging based surrogate modeling for fractional order control of microgrids. *IEEE Trans Smart Grid* 6(1):36–44
10. Sahoo BP, Panda S (2018) Improved grey wolf optimization technique for fuzzy aided PID controller design for power system frequency control. *Sustain Energy Grids Netw* 16:278–299
11. Padhan S, Sahu RK, Panda S (2014) Application of firefly algorithm for load frequency control of multi-area interconnected power system. *Elect Power Compon System* 42(13):1419–1430
12. Nguyen GN, Jaatheesan K, Ashour AS, Anand A, Dey N (2017) Ant colony optimization based load frequency control of multi-area interconnected thermal power system with governor dead-bands nonlinearity. *Smart Trends Syst Secur Sustain* 18:633–638
13. Sahu RK, Panda S, Rout UK, Sahoo DK (2016) Teaching learning-based optimization algorithm for automatic generation control of power system using 2-DOF PID controller. *Int J Electr Power Energy Syst* 77:287–301
14. Panda S, Yegireddy NK (2013) Automatic generation control of multi-area power system using multi-objective non-dominated sorting genetic algorithm-II. *Int J Electr Power Energy Syst* 53:54–63
15. Kennedy J, Eberhart R (1995) Particle swarm optimization. In: *Proceedings of Int. Conf. on Neural Networks*, Perth, WA, Australia, vol. 4, pp. 1942–1948
16. Storn R, Price K (1997) Differential evolution—a simple and efficient heuristic for global optimization over continuous spaces. *J Global Optim* 11(4):341–359
17. Rout UK, Sahu RK, Panda S (2013) Design and analysis of differential evolution algorithm based automatic generation control for interconnected power system. *Ain Shams Eng J* 4(3):409–421
18. Sahu RK, Panda S, Padhan S (2015) A hybrid firefly algorithm and pattern search technique for automatic generation control of multi area power systems. *Int J Electr Power Energy Syst* 64:9–23
19. Kassem AM, Abdelaziz AY (2015) BFA optimization for voltage and frequency control of a stand-alone wind generation. *Electr Eng Unit* 97(4):313–325
20. Sahu RK, Rout UK, Panda (2013) Sensitivity Analysis of Load-Frequency Control of Power System Using Gravitational Search Algorithm. In: *Proceedings of Int. Conf. on Frontiers of Intelligent Computing: Theory and Applications*, pp. 249–258
21. Barik AK, Das DC (2019) Coordinated regulation of voltage and load frequency in demand response supported bio-renewable cogeneration-based isolated hybrid microgrid with quasi-oppositional selfish herd optimisation. *Int Trans Electr Energy Syst*. <https://doi.org/10.1002/2050-7038.12176>
22. Bhuyan M, Barik AK, Das DC (2020) GOA optimised frequency control of solar-thermal/sea-wave/biodiesel generator based interconnected hybrid microgrids with DC link. *Int J Sustain Energy*. <https://doi.org/10.1080/14786451.2020.1741589>
23. Singh A, Suhag S (2019) Frequency regulation in an AC microgrid interconnected with thermal system employing multiverse optimized fractional order-PID controller. *Int J Sustain Energy* 39:1–13
24. Kumar B, Bhongade S (2016) Load disturbance rejection based PID controller for frequency regulation of a microgrid. In: *Proceedings of Int. Conf. on Power and Energy Systems: Towards Sustainable Energy*, Bangalore, pp 1–6
25. Mishra S, Malleshm G, Sekhar PC (2013) Biogeography based optimal state feedback controller for frequency regulation of a smart microgrid. *IEEE Trans Smart Grid* 4(1):628–637
26. Kumar B, Bhongade S (2017) Load disturbance rejection based PID controller for frequency regulation of a microgrid. *Indones J Electr Eng Comput Sci* 7(3):625–642
27. Mishra SS, Mishra SK, Swain SK (2017) Coefficient diagram method (CDM) based PID controller design for magnetic levitation system with time delay. In: *Proceedings of IEEE Int. Conf. on Intelligent Techniques in Control, Optimization and Signal Processing*, Srivilliputhur, pp 1–8
28. Mohamed TH, Shabib G, Ali H (2016) Distributed load frequency control in an interconnected power system using ecological technique and coefficient diagram method. *Electr Power Energy Syst* 82:496–507
29. Manabe S (1998) The coefficient diagram method. In: *14th IFAC symposium on Automatic control in aerospace*, pp 24–28
30. Bhaba PK, Somasundaram S (2009) Real time implementation of a new CDM-PI control scheme in conical tank liquid maintaining system. *CCSE Modern Appl Sci* 3(5):38–45
31. Somasundaram S, Bhaba PK (2010) Control of bioreactor process using a new CDM-PID control strategy. *J Eng Sci Technol* 5(3):213–222
32. Thuengsripan S, Suksri T, Numsomran A, Kongratana V, Roengruen P (2007) Smith predictor design by CDM for temperature control system. In: *Proceedings of Int. Conf. on Control, Automation and Systems*, Seoul
33. Kalpana K, Meenaakshipriya B (2014) Design of coefficient diagram method (CDM) based PID controller for double integrating unstable system. In: *Proceedings of IEEE Int. Conf. on Electrical Engineering Systems*, Chennai, India
34. Imal E (2009) CDM based controller design for nonlinear heat exchanger process. *Turk J Electr Eng Comput Sci* 17(2):143–161
35. Somasundaram S, Bhaba PK (2009) A new CDM PIPD control strategy for unstable process. *Int J Eng Simul* 10(1):19–24
36. Manabe S (2003) Importance of coefficient diagram in polynomial method. In: *Proceedings of IEEE Int. conf. on decision and control*, Maui, HI, USA, December 2003
37. Raj R, Anand LDV (2013) Design and implementation of a CDM-PI controller for a spherical tank level system. *Int J Theor Appl Res Mech Eng* 2(1):49–52
38. Mirjalili S, Mirjalili SM, Lewis A (2014) Grey wolf optimizer. *Adv Eng Softw* 69:46–61
39. Padhy S, Panda S, Mahapatra S (2017) A modified GWO technique-based cascade PI-PD controller for AGC of power systems in presence of plug in electric vehicles. *Eng Sci Technol* 20(2):427–442
40. Kumar B, Adhikari S, Datta S, Sinha N (2019) Real time simulation of modified bias based load disturbance rejection controller for frequency regulation of islanded micro-grid. *Int J Emerg Electr Power Syst* 20(5):1–13
41. Guha D, Roy PK, Banerjee S (2016) Load frequency control of interconnected power system using grey wolf optimization. *Swarm Evol Comput* 27:97–115
42. Kundur P (2009) *Power system stability and control*. Tata McGraw-Hill, New Delhi
43. Elgerd OI (2007) Chapter 6. In: *Electric energy systems theory: an introduction*. Tata McGraw-Hill Publishing Company Ltd, New Delhi

Publisher's Note Springer Nature remains neutral with regard to jurisdictional claims in published maps and institutional affiliations.

Badal Kumar received B.Tech degree in Electrical and Electronics Engineering from Biju Patnaik University of Technology, Orissa and Master's in Digital Technique and Instrumentation, S.G.S Institute of Technology and Science, Indore, India in 2011 and 2015 respectively. He had joined as a faculty in the Department of Electrical and Electronics Engineering, Oriental College of Technology, Bhopal, India in

Aug. 2015. He joined MEDI-CAPS University, Indore as an assistant professor in the Department of Electrical Engineering in 2017. Currently, he is pursuing Ph.D. from National Institute of Technology, Manipur. His areas of interest include micro grid, smart grid, control system application in different areas, power system operation and control, renewable energy sources.

Shuma Adhikari received B.Tech., M.Tech. and Ph.D degrees from NIT Agartala (India), NIT Silchar (India) and NIT Manipur (India) in 2008, 2010 and 2017 respectively. She is currently working as an Assistant Professor in Department of Electrical Engineering, NIT Manipur, India. Her research Interests includes power system protection, Micro-grid and FACTs devices.

Subir Datta received his B.Tech. from NERIST, India in 2008; M.Tech. and PhD Degrees from NIT Silchar, India in 2010 and 2017 respectively. He is currently an Assistant Professor in the Department of

Electrical Engineering, Mizoram University, India. His research interests include FACTS, electric machine and drives, renewable energy, AC and DC micro grid and power electronics.

Nidul Sinha received B.E. degree in Electrical Engineering from Calcutta University India in 1984. He obtained his M.Tech. Degree from IIT, Delhi, India in 1989 and Ph.D. degree from Jadavpur University, Kolkata, India. He worked in Calcutta Port Trust as a trainee before joining as a lecturer in Regional Engineering College (now NIT Silchar) in 1985. His research interests include power system optimization, deregulation, power system control, wind energy and induction generators, automatic generation control of interconnected systems, soft computing techniques and applications, micro grid. He is a reviewer of IEEE PWRS, PWRD, PESL, IEE part-c, EPSR, and DSP (Elsevier).